

On the Effects of Dissipative Turbulence on the Narrow Emission-Line Ratios in Seyfert Galaxies

S.B. Kraemer^{1,2}, M.C. Bottorff³, & D.M. Crenshaw⁴

ABSTRACT

We present a photoionization model study of the effects of micro-turbulence and dissipative heating on emission lines for number and column densities, elemental abundances, and ionizations typical for the narrow emission line regions (NLRs) of Seyfert galaxies. Earlier studies of NLR spectra generally found good agreement between the observations and the model predictions for most strong emission lines, such as [O III] λ 5007, [O II] λ 3727, [N II] λ 6583, [Ne III] λ 3869, and the H and He recombination lines. Nevertheless, the strengths of lines from species with ionization potentials greater than that of He⁺ (54.4 eV), e.g. N⁺ and Ne⁺, were often under-predicted. Among the explanations suggested for these discrepancies were (selectively) enhanced elemental abundances and contributions from shock heated gas. Interestingly, the NLR lines have widths of several 100 km s⁻¹, well in excess of the thermal broadening. If this is due to micro-turbulence, and the turbulence dissipates within the emission-line gas, the gas can be heated in excess of that due to photoionization. We show that the combined effects of turbulence and dissipative heating can strongly enhance N V λ 1240 (relative to He II λ 1640), while the heating alone can boost the strength of [Ne V] λ 3426. We suggest that this effect is present in the NLR, particularly within \sim 100 pc of the central engine. Finally, since micro-turbulence would make clouds robust against instabilities generated during acceleration, it is not likely to be a coincidence that the radially outflowing emission-line gas is turbulent.

Subject headings: galaxies: Seyfert – line formation – turbulence

¹Institute for Astrophysics and Computational Sciences, Department of Physics, The Catholic University of America, Washington, DC 20064; kraemer@yancey.gsfc.nasa.gov

²Astrophysics Science Division, Code 667, NASA's Goddard Space Flight Center, Greenbelt, MD 20771

³Physics Dept., Southwestern University, FJS123, 1001 E. University Ave., Georgetown, TX 78626

⁴Department of Physics and Astronomy, Georgia State University, Atlanta, GA 30303

1. Introduction

Seyfert galaxies are relatively nearby ($z < 0.1$), low-luminosity (bolometric luminosities $L_{\text{bol}} < 10^{45}$ erg s $^{-1}$) examples of Active Galactic Nuclei. Based on the widths of their optical emission lines, Seyfert galaxies are generally divided into two types (Khachikian & Weedman 1971). Seyfert 1 galaxies possess broad permitted lines, with full width at half-maxima (FWHMs) $\geq 10^3$ km s $^{-1}$, narrower forbidden lines, with FWHM ~ 500 km s $^{-1}$, and optical continua which are dominated by non-stellar emission (e.g., Oke & Sargent 1968). Seyfert 2 galaxies show only narrow emission lines and the non-stellar contribution to their optical continua is much weaker (Koski 1978). The broad emission lines in Seyfert 1s vary on short timescales in response to changes in the continuum flux, which indicates that this emission arises in dense gas within tens of light-days of the central source (e.g. Peterson et al. 2004), in what is referred to as the Broad Line Region (BLR). The narrow lines detected in both Seyfert 1s and 2s can extend ~ 1 kpc from the AGN (e.g. Schmitt & Kinney 1996; Schmitt et al. 2003), forming the so-called Narrow-Line Region (NLR). Spectropolarimetry studies revealed the presence of strongly polarized continua and broad permitted line emission in several Seyfert 2 galaxies. This discovery led to the unified model for Seyfert galaxies (Antonucci 1993), which posits that the differences between the two types is the result of viewing angle, with Seyfert 2 galaxies characterized by the obscuration of their broad-lines regions and central engines by a dusty circumnuclear torus. In this model, the torus collimates the ionizing radiation and the resulting illumination pattern produces a roughly biconical NLR (Schmitt & Kinney 1996). If the AGN is viewed at high inclination, the bicone axis is roughly in the plane of the sky, maximizing the projected angular size of the NLR.

While historically there has been some debate about the importance of collisional and/or shock ionization of the NLR (e.g., Kriss et al. 1992; Wilson & Raymond 1999), the narrowness of Radiative Recombination Continua detected in XMM-*Newton* spectra (Sako et al. 2000; Kinkhabwala et al. 2002; Turner et al. 2003; Armentrout, Kraemer, & Turner 2007) is a clear indication that the emission-line gas is photoionized by the central source. We have analyzed *Hubble Space Telescope (HST)*/Faint Object Spectrograph (FOS) observations of the NLR in the Seyfert 1 galaxies NGC 5548 (Kraemer et al. 1998a) and NGC 4395 (Kraemer et al. 1999), and the Seyfert 2 galaxy NGC 1068 (Kraemer, Crenshaw & Ruiz 1998b) and *HST*/Space Telescope Imaging Spectrograph (STIS) observations of NGC 1068 (Kraemer & Crenshaw 2000a, 2000b), the Seyfert 1 galaxy NGC 4151 (Nelson et al. 2000; Kraemer et al. 2000), and the Seyfert 2 galaxy Mrk 3 (Collins et al. 2005). The STIS observations were obtained in the low-resolution/long slit mode (see Woodgate et al. 1998), with which we were able to spatially resolve the NLRs and explore the nature of the emission-line clouds as a function of distance from the central sources. Using photoionization models, we were

able to constrain the densities, column densities, dust/gas ratios, and ionization state of the emission-line gas. In general, we were able to fit nearly all of the observed emission line fluxes and ratios by assuming the gas was photoionized solely by the central source. Nevertheless, we found discrepancies in the predicted strengths of a few emission lines, typically those from the higher ionization states (i.e., those with ionization potentials above the He II Lyman limit), such as N V $\lambda 1240$ ¹, [Ne V] $\lambda\lambda 3346, 3426$, and [Fe VII] $\lambda 6087$. Usually, our models under-predicted the strengths of these lines by factors of ~ 2 , although the discrepancies were often much greater for N V. The poor fit to high-ionization lines was also noted by Oliva (1997), and may be rectified by adjusting the elemental abundances or including additional ionization/excitation mechanisms (e.g. Kriss et al. 1992). In the modeling of the NLR emission in NGC 5548 (Kraemer et al. 1998a) and NGC 1068 (Kraemer et al. 1998b), we were able to improve the fit for the N V and [Ne V] lines by assuming super-solar abundances of nitrogen and neon. However, including higher abundances for selected elements resulted in over-predictions of lines from lower ionization states, e.g. N IV] $\lambda 1486$. Indeed, in most cases, the strengths of the lower ionization lines from these elements, e.g., [Ne III] $\lambda 3869$ and [N II] $\lambda\lambda 6548, 6583$, are consistent with roughly solar abundances (see Section 2.1).

In addition to photoionization model studies of the NLR, we have also used spatially resolved STIS spectra to analyze the kinematics of the emission-line gas in NGC 1068 (Crenshaw & Kraemer 2000; Das et al. 2006), Mrk 3 (Ruiz et al. 2001, 2005) and NGC 4151 (Crenshaw et al. 2000; Das et al. 2005). Although the kinematic studies utilized the [O III] $\lambda 5007$ line, we have found that the higher ionization lines are spatially co-located with the [O III] knots (e.g. Collins et al. 2005), therefore it is probable that similar dynamical effects drive the higher ionization gas. Each of these sources show a similar kinematic profile, in which the projected radial velocity, v_r , gradually increases from the central point source out to $r \sim 100$ pc, after which the velocities abruptly begin to decrease towards systemic. We have been able to model the kinematics by assuming the gas is confined to a hollow, bi-conical envelope, whose apex is roughly coincident with the AGN. The gas is continuously accelerated, then begins to undergo a rapid deceleration. The dynamics of this process is still not clear (e.g. Everett & Murray 2006; Das, Crenshaw, & Kraemer 2007), but it is likely that radiation pressure from the continuum source makes an important contribution. The [O III] lines are also quite broad in these objects, e.g., FWHM > 1000 km s⁻¹ near the apex of the bicone and $\gtrsim 500$ km s⁻¹ throughout the inner 200 pc of the NLR. In general,

¹For both the observations and the models, we consider the combined N V $\lambda\lambda 1238.8, 1242.8$ (N V $\lambda 1240$) and C IV $\lambda\lambda 1548.2, 1550.8$ (C IV $\lambda 1550$), since the doublets were not resolved in the FOS and low-resolution STIS spectra.

the widths appear to decrease with distance from the AGN, although there are points of abrupt increases, particularly in the case of NGC 1068 (Crenshaw & Kraemer 2000; Das et al. 2006), which occur near the velocity turn-over points. The physical conditions that produce these line widths is unclear (see Section 5.). It is possible that they result from the super-position of multiple individual kinematic components; if so, the flow may simply become more chaotic at the turn-over points, broadening the profiles. However, it is also possible that the emission-line knots possess significant micro-turbulence. Whatever process slows the knots could conceivably boost the micro-turbulence. Another piece of evidence that the outflowing gas is turbulent is found in the blue-shifted UV absorption detected along the line-of-sight to many Seyfert 1 galaxies (Crenshaw et al. 1999; Crenshaw, Kraemer, & George 2003; Dunn et al. 2007). The absorption lines nearly always have widths ($>$ tens of km s^{-1}) in excess of thermal (\sim several km s^{-1}) and, in several cases, we have measured FWHMs $>$ several hundred km s^{-1} (e.g. Kraemer et al. 2001). The absorption lines appear/disappear over short timescales (e.g. Crenshaw & Kraemer 1999; Kraemer, Crenshaw, & Gabel 2001; Crenshaw et al. 2003) without obvious changes in their widths, which is suggestive of turbulent knots passing across our line-of-sight.

In Figures 1 – 3, we show the N V $\lambda 1240$ /He II $\lambda 1640$, C IV $\lambda 1550$ /He II $\lambda 1640$, and [Ne V] $\lambda 3426$ /He II $\lambda 1640$ ratios as a function of projected radial distance, r , and FWHM. There is some evidence for higher values at $r \lesssim 100$ pc, although there are some points with high ionization ratios at greater radial distances for C IV and [Ne V]. More evident is the correlation of the line ratios with FWHM. If the broader lines are found in more highly excited components, as the ratios indicate, it suggests some physical connection. Therefore, our hypothesis is that the line widths result, at least partly, from internal micro-turbulence, which in turn affects the observed line ratios.

A related issue is that the broad emission lines in AGN are smooth (e.g., Dietrich, Wagner, & Courvoisier 1999). If the lines are thermally broadened, there must be an inordinately large number of individual clouds within the BLR. To address this problem, Bottorff & Ferland (2000) proposed that the clouds are internally turbulent, with micro-turbulent velocities that exceed their thermal velocities. Using photoionization models, they were able to generate smooth line profiles from a small number of clouds. Bottorff & Ferland (2002, hereafter BF2002) expanded on this by examining the effects of dissipative turbulence. In the case of non-dissipative turbulence, the turbulent motions persist, whereas, in the dissipative case, the motion is converted into heat. The corresponding increase in electron temperature will affect the emissivity of emission lines, particularly those that are collisionally excited. There is evidence for dissipative heating in the diffuse interstellar medium of the Milky Way Galaxy (Minter & Balser 1997), hence BF2002 argued that such processes were likely to occur within the BLR gas in AGN. Since the thermal motions will decay due to the heating losses,

there must be some continual external source of turbulence. Possibilities include the intense radiation pressure experienced by gas close to the AGN and magnetic fields. Interestingly, both radiation pressure and magneto-hydrodynamic (MHD) Flows have been suggested as mechanisms for mass loss in AGN (see Crenshaw et al. 2003, and references therein), hence it is possible that forces that drive the outflows also maintain the micro-turbulence.

BF2002 parameterized the dissipative heating as a function of turbulence velocity, as follows:

$$Q = \eta_v \rho \frac{v_t^3}{D} \text{ergs cm}^{-3} \text{ s}^{-1}, \quad (1)$$

where η_v is of order unity (see Stone, Ostriker, & Gammie 1998), v_t is the magnitude of the turbulence velocity², ρ is the mass density of the gas, and D is the scale length over which the turbulence dissipates. BF2002 assumed that D corresponds to the physical depth of a BLR cloud, or $\sim 10^{13}$ cm, based on typical BLR hydrogen number densities ($n_H \sim 10^{10}$ cm⁻³; Davidson & Netzer 1979) and column densities ($N_H \sim 10^{23}$ cm⁻²; Kwan & Krolik 1981). For their models, they re-parameterized the heating rate as: the following:

$$Q \approx 2.3 \times 10^{-3} v_3^3 \frac{n_{10}}{L_{13}} \text{ergs cm}^{-3} \text{ s}^{-1}, \quad (2)$$

where v_3 is the turbulence velocity in units of 1000 km s⁻¹, n_{10} is the hydrogen number density in units of 10¹⁰ cm⁻³, L_{13} is the physical depth of the cloud, in units of 10¹³ cm. In this paper, we examine the effects of dissipative turbulence in the NLR gas and have used equation (2) to calculate the heating. Following BF2002, we assumed that the turbulence dissipates over the full depth of the cloud. However, although the column densities of NLR tends to be much lower than the canonical BLR value (Kraemer et al. 1998a, 1998b; Kraemer et al. 2000, Kraemer & Crenshaw 2000a, 2000b), the physical depths are several orders of magnitude larger, due to the much lower densities.

2. Photoionization Modeling

We have calculated a set of photoionization models to investigate the effects of micro-turbulence and dissipative heating on the NLR emission-line ratios. The elemental abundances and other model input parameters are detailed in the next two subsections.

²The turbulence velocity is equivalent to the velocity dispersion, $\sigma(v)$, which is 1/2.355 times the Full Width Half Maximum (FWHM) of a Gaussian line profile.

2.1. Elemental Abundances

The relative strengths of emission lines strongly depend on the elemental abundances. Since the thermal equilibrium in the optical emission-line gas is driven largely by collisional cooling, the electron temperature is quite sensitive to the relative fraction of heavy atoms (neutral and ionized) in gas phase. For example, for heavy-element abundances more than several times solar values, the collisionally excited lines can actually be weaker than for lower abundances due to the increased line-cooling rates. While the abundances of common elements such as C, O, and Ne scale with Z/Z_{\odot} (where Z_{\odot} indicates “solar abundances”), N scales as $(Z/Z_{\odot})^2$ (e.g., Vila-Costas & Edmunds 1993). Hence, N/C-O-Ne can become quite large at super-solar abundances, which should result in the enhancement of lines such as N V λ 1240 and the N IV] λ 1486 multiplet compared to lines from these other elements.

In our previous NLR studies (see Section 1), we have assumed “roughly solar” abundances (e.g. Grevesse & Anders 1989). Recently, Groves, Dopita, & Sutherland (2004) re-visited the issue of elemental abundances in the NLR, and incorporated the latest efforts to define solar abundances (e.g. Grevesse & Sauval 1998), which suggested somewhat lower N/H than previous studies. In order to reproduce the observed strengths of the [N II] $\lambda\lambda$ 6548,6583 lines with their photoionization models, Groves et al. had to assume twice the solar N/H ratio (interestingly, this is quite close to “roughly” solar value that we had used in our previous NLR modeling). It is worth noting that similarly elevated abundances were determined for the blue-shifted UV absorbers in the Seyfert 1 galaxy Mrk 279 (Arav et al. 2007), particularly since the UV absorbers and the emission-line gas in the inner NLR may be associated (Crenshaw & Kraemer 2005). Assuming all the elements have scaled together, this corresponds to a overall abundance of $Z/Z_{\odot} \approx 1.4$. For this paper, we used the abundances from Asplund, Grevesse, & Sauval (2005), scaled in manner suggested by Groves et al. The logs of the abundances relative to H by number are: He: -1.0 ; C: -3.46 ; N: -3.92 ; O: -3.19 ; Ne: -4.01 ; Mg: -4.33 ; Si: -4.34 ; S: -4.69 ; Fe: -4.5 . Note that the Ne/O ratio is ~ 0.15 , in agreement with current estimates that include the effect of solar CNe mixing (see Delahaye & Pinsonneault 2006).

Although much of the NLR gas may be dusty (Kraemer & Harrington 1986; Groves et al. 2004) we have not included dust in these models. The reasoning is twofold. First, there would be no depletion of neon and little if any of nitrogen (in the absence of ice mantles) onto grains. Second, we have found evidence that the dust/gas ratios in the NLR are below that of the ISM and, in some cases (e.g. NGC 1068: Kraemer & Crenshaw 2000a), the gas in the inner NLR appears to be dust-free.

2.2. Model Input Parameters

The photoionization models used for this study were generated using the Beta 5 version of Cloudy (Ferland et al. 1998). As per convention, the models are parameterized in terms of the ionization parameter, $U = Q/(4\pi r^2 c n_H)$ where r is the distance between the emission-line gas and the central source, n_H is the hydrogen number density, c is the speed of light, and $Q = \int_{13.6\text{eV}}^{\infty} (L_\nu/h\nu) d\nu$, or the number of ionizing photons s^{-1} emitted by a source of luminosity L_ν $\text{ergs s}^{-1} \text{Hz}^{-1}$. We assumed a plane-parallel (“slab”) geometry. For the incident continuum, we used the spectral energy distribution which we employed in our modeling of NGC 4151 (Kraemer et al. 2005), which is parameterized as a broken power law of the form $L_\nu \propto \nu^\alpha$ as follows: $\alpha = -1.0$ for energies < 13.6 eV, $\alpha = -1.45$ over the range $13.6 \text{ eV} \leq h\nu < 0.5 \text{ keV}$, and $\alpha = -0.5$ above 0.5 keV. We included a low energy cut-off at 1.24×10^{-3} eV (1 mm) and a high energy cutoff at 100 keV. While we compare our model predictions with emission-line spectra from other Seyfert galaxies, the results were not sensitive to small changes in the power-law indices or break energies, and using a single model SED makes comparison of the model predictions to the complete set of emission-line ratios more straightforward.

Based on our previous models, NLR gas within a few tens of pcs of the AGN can be characterized assuming $n_H = 10^5 \text{ cm}^{-3}$. The line ratios of interest to this study do not change appreciably for lower values of n_H , and the value used is well below the critical density for the 1D_2 level of Ne V (the upper level of the 3426 Å transition; Osterbrock 1989). We assumed $N_H = 10^{21} \text{ cm}^{-2}$, which is consistent with matter-bounded clouds over the range of ionization we used, i.e., $-2 \leq \log(U) \leq 0$. Based on n_H and N_H , the physical depth for the model clouds was 10^{16} cm. The turbulence velocity, v_t , is directly command-able in Cloudy (Ferland et al. 1998). The dissipative heating, based on the density, physical depth and v_t (see Table 1), was introduced via the command-able additional heating term. We examined the effects of turbulence and dissipative heating for a range of v_t from 0 (thermal broadening only) to 250 km s^{-1} .

3. Model Results

In our models, we tested the effects of turbulence/heating on two emission lines that are strong and often under-predicted by photoionization models: N V $\lambda 1240$ and [Ne V] $\lambda 3426$. As shown in Figure 4, the He^{+2} zone, in which there is the strongest contribution to the He II recombination lines, is coincident with the N^{+4} and Ne^{+4} zones. Therefore, the results are given as line ratios relative to the He II $\lambda 1640$ recombination line.

For resonance lines such as N V $\lambda 1240$, there can be a contribution from photo-excitation to the upper level by continuum radiation. This has been suggested as the mechanism responsible for the strong resonance lines from He-like and H-like ions of Ne, O, and N detected in X-ray spectra of Seyfert galaxies (e.g. Sako et al. 2000; Kinkhabwala et al. 2002; Armentrout et al. 2007). If the gas is turbulent, the absorption profiles are broadened, which increases the number of continuum photons that the gas can absorb before becoming optically thick to the incident radiation, thereby increasing the contribution from photo-excitation. To test the effect of photo-excitation alone, we generated a set of models with turbulence but no dissipative heating. The results for N V are shown in Figure 5. In the absence of turbulence, the maximum N V/He II ratio is ~ 1.4 , which occurs near an ionization parameter of $\log(U) = -0.4$. The N V/He II ratio increases with turbulence, reaching a value of ~ 4 for $v_t = 250 \text{ km s}^{-1}$. The shape of the turn-over at $\log(U) > -0.4$ depends on the predicted He II $\lambda 1640$, which is relatively stronger at high turbulence as the model diverges from the Case B approximation (e.g. Osterbrock 1989). Therefore, elevated N V/He II ratios can be achieved for large micro-turbulence, although there is no effect on forbidden lines such as [Ne V] $\lambda 3426$. However, the range in ionization parameter for which N V/He II ratios > 2 are predicted is rather narrow and covers a range for which the gas is so highly ionized that most of the nitrogen is in higher ionization states than N^{+4} . The N V is enhanced in this case because the smaller N^{+4} column densities result in lower N V optical depths. The effect of turbulence alone is not as strong at the ionization parameter at which the largest column density of N^{+4} is predicted, $\log(U) \approx -1.3$, since the line becomes optically thick close to the irradiated face of the slab. Also, the NLR must include gas at lower ionization, which still produces He II emission, hence the contribution from turbulent gas with high N V/He II ratios will be diluted. Therefore, photo-excitation, even when maximized by high turbulence, may not be sufficient to produce the highest observed NV /He II ratios (see Figure 1), unless the nitrogen abundances are \gtrsim several times solar.

The effect of dissipative heating scaled with micro-turbulence on the N V/He II ratio is shown in Figure 6. The peak ratio increases with heating, peaking at ~ 11 for $v_t = 250 \text{ km s}^{-1}$. Comparing these results to the models generated without heating, in addition to predicting high ratios over a broader range of ionization parameter, the ionization parameters at which N V/He II peaks drop with increased heating/turbulence. This demonstrates the relative contributions from photo-excitation and dissipative heating: when heating is included, there is a significant enhancement of the line in the more optically thick models, and the heating becomes the dominant effect for $v_t > 200 \text{ km s}^{-1}$. Including heating has a significant effect on the [Ne V]/He II ratio, as well, as shown in Figure 7. The slight trend to lower values of U for the peak ratio is due to the higher electron temperatures for the models with the greatest Ne^{+4} fraction. As these results indicate, [Ne V]/He II ratios greater than

unity require the heating resulting from $v_t > 100 \text{ km s}^{-1}$.

Since we have included dissipative heating, we examined the thermal stability of the gas. The thermal stability curves (e.g., Krolik, McKee, & Tarter 1981) are shown in Figure 8. Although the unstable region, characterized by negative slope, is more pronounced for the models with $v_t = 250 \text{ km s}^{-1}$, the gas will be thermally stable for the range of ionization parameters from which we examined emission-line ratios, i.e., $\log(U) < 0.0$.

4. Comparison with Observations

Since the under-prediction of the N V/He II and [Ne V]/He II ratios is the motivation for this study, we now demonstrate to what degree the addition of dissipative heating can reduce these discrepancies. As discussed in Section 1, kinematic studies have found that the [O III] $\lambda 5007$ lines in the NLR can be broad. For example, the brightest components in NGC 1068 typically have FWHM of $\lesssim 700 \text{ km s}^{-1}$ (Das et al. 2006), while those in NGC 4151 have FWHM of $\lesssim 500 \text{ km s}^{-1}$ (Das et al. 2005). Also, the largest FWHM detected among the strong UV absorption components in NGC 4151 is $\approx 435 \text{ km s}^{-1}$ (Kraemer et al. 2001). In order to test the effects of micro-turbulence, we have opted to be somewhat conservative and have generated models with turbulence velocities of, 50, 100, and 150 km s^{-1} (which corresponds to FWHM $\approx 120, 235, \text{ and } 350 \text{ km s}^{-1}$) for comparison to the observed line ratios. The values assumed for U , N_H , and n_H are as described in Section 2.2.

In Figure 9, we compare the model predictions for N V $\lambda 1240$ /He II $\lambda 1640$ versus [Ne V] $\lambda 3426$ /He II $\lambda 1640$ against the observations. Although there are a large number of datapoints for which both the N V and [Ne V] lines are relatively weak, it is apparent that turbulence combined with dissipative heating is required for those points with N V/He II > 1.5 and [Ne V]/He II > 0.5 . The few points that lie outside the upper ($v_t = 150 \text{ km s}^{-1}$) curve could be matched by higher turbulence/heating. In particular, note the datapoint for NGC 5548. In Kraemer et al. (1998a), we had suggested that the large N V/He II and [Ne V]/He II ratios in the source might be the result of a high nitrogen and neon abundances. However, these results suggest that strong N V and [Ne V] lines are more likely indicative of turbulence/heating.

In Figure 10, we show the model predictions for N V/He II versus C IV $\lambda 1550$ /He II $\lambda 1640$. The model comparison shows that C IV/He II ratios > 4 are consistent with turbulence/heating. We also compared the N V/He II is to N IV] $\lambda 1486$ /He II. While the number of datapoints was small due to the relative weakness of N IV], combined with the effects of reddening, there is some indication that the N IV] may show the effects of dissipative

heating.

An additional indication that the NLR gas is turbulent is that high $L\beta/L\alpha$ ratios have been detected in some Seyferts. In *Hopkins Ultraviolet Telescope* spectra of NGC 1068, Kriss et al. (1992) measured a ratio of ~ 0.1 , while, under Case B conditions (Osterbrock 1989), this ratio will be $\ll 0.01$. In our models, we find that for $\log(U) = 1.5$, without turbulence, $L\beta/L\alpha \approx 1.4 \times 10^{-3}$. For $v_t = 150 \text{ km s}^{-1}$, the ratio is ≈ 0.01 . Decreasing the column density by a factor of 10 increases $L\beta/L\alpha$ by a similar factor. Hence, this strongly suggests that the gas in the NLR is turbulent, although the column densities of the Lyman-emitting gas may be somewhat lower than those assumed here, but well-within the range of values used in our previous NLR studies (e.g. Kraemer et al. 2000; Kraemer & Crenshaw 2000b).

5. Discussion

The inclusion of micro-turbulence with associated dissipative heating has the effect of increasing the strengths of the NV and [NeV] lines, relative to HeII. In the range of ionization parameter for which these lines are strongest, i.e. $-1.5 < \log(U) < -1.3$, the volume heating rate for a turbulence velocity = 150 km s^{-1} is on the same order as the radiative heating rate. Spatially resolved spectra of the NLR of Seyferts (see Section 1) reveal that the emission-line knots remain quite broad (FWHM $>$ several hundred km s^{-1}) throughout the inner $\sim 200 \text{ pc}$ of the NLR. This suggests that if this is due to micro-turbulence, the turbulence is being continuously driven, perhaps by the continuum radiation from the central source. For example, in NGC 4151, which has a luminosity in ionizing photons of $\sim 10^{53} \text{ photons s}^{-1}$ (Kraemer et al. 2005), an emission-line cloud, characterized by $\log(U) = -1.5$, $n_H = 10^5 \text{ cm}^{-3}$, and $N_H = 10^{21} \text{ cm}^{-2}$, would lie at $r = 9.2 \times 10^{18} \text{ cm}$. If this gas formed a complete shell around the central source, to produce the dissipative heating rate assumed in our models (see Table 1) would require an energy input rate of $8.2 \times 10^{41} \text{ erg s}^{-1}$, which is a fraction of the bolometric luminosity of NGC 4151, even during the low-flux state observed in 2002 May ($L_{bol} \approx 5 \times 10^{43} \text{ erg s}^{-1}$; Kraemer et al. 2005). Therefore, *based on the energetics*, it is possible that the continuum radiation can continuously drive the micro-turbulence.

Since the emission-line gas is part of a radial outflow, one must consider possible connections between the line widths and the means by which the gas is accelerated. Various mechanisms have been suggested for the acceleration including radiation pressure (Blumenthal & Mathews 1975; Mathews 1976), ram pressure from winds (Weymann et al. 1982; Schiano 1986; Smith 1993) and MHD-driven flows (Blandford & Payne 1982; Bottorff, Korista, & Shlosman 2000). A Blandford & Payne type MHD wind has (in cylindrical coordinates, r, z, ϕ) a z -component of outflow velocity that increases monotonically, but the r - and ϕ -

velocity components can rapidly increase (e.g., in the BLR) but then decrease further out (e.g., in the NLR). Therefore it is possible to have large NLR line widths near the base and small line widths far from the base that have nothing to do with turbulence or an outwardly propagating disturbance. Our kinematic studies have shown that the emission-line gas is accelerated to velocities $\sim 1000 \text{ km s}^{-1}$ within the inner 100 pc of the NLR. Over the same distance scales, the FWHM of the lines decrease from 1000 km s^{-1} to a few hundred km s^{-1} (with some notable exceptions). Although this is consistent with super-position of velocity components, taken together with the correlation between the N V/He II, C IV/He II, and [Ne V]/He II ratios and FWHM of these lines, we interpret this as evidence that it is turbulence (largely) and not systematic non-radial components of the outflow that contribute to the line widths.

While a cloud of gas is being accelerated, the driving mechanism will generate instabilities within the cloud, such as Rayleigh-Taylor, for a radiatively driven cloud, or Kelvin-Helmholtz instabilities, for a cloud entrained in a wind. If the timescale for the instability to propagate through the cloud is less than the timescale for acceleration, e.g. to achieve the observed radial velocities, the cloud will fragment. It has been shown (e.g. Allen 1984; Smith 1993) that fragmentation is inevitable for clouds with physical parameters similar to those derived from our photoionization models (which are the basis for the range in parameters assumed in this paper). There are only two ways to reconcile this. One way is for the clouds to constantly form and evaporate within a hot wind (e.g. Krolik & Kriss 2001). The other way is for the clouds to be robust to instability-driven fragmentation via internal turbulence (Allen 1984). The turbulence could be generated by multiple shocks which also accelerate the clouds (Marscher 1978). Interestingly, this requires turbulence velocities $0.1v_r < v_t < v_r$, which is consistent with observations; for $v_t > v_r$, the clouds will evaporate. Marscher (1978) further notes that stable clouds must have radii $> 10^{14} \text{ cm}$, which is consistent with our modeling results.

Micro-turbulence in NLR clouds will dissipate into heat on a time scale shorter than the NLR crossing time. This means that energy must be provided constantly to drive the turbulence. As mentioned above it is energetically possible for the continuum to do this. However transferring the energy into turbulent motions at the required rate may more problematic. If the outflow is an MHD wind magnetic field lines which thread NLR clouds also thread the portion of the disk from which the NLR material was originally launched. This provides a possible energy conduit to the NLR clouds. It is uncertain however whether disturbances launched from the disk could travel over a distance of 100 pc to be dissipated in NLR clouds. A combination of radiative driving and an MHD wind however offers the possibility that NLR materials can be driven against magnetic field lines thereby exciting disturbances which would dissipate more or less locally as heating. Such a mechanism is an

area for future study. At the very least the presence of magnetic fields may be necessary to avert overly strong shock formation in the highly turbulent gas.

Therefore, we suggest the following scenario. The emission-line clouds form relatively close to the central source, perhaps in the inner few pcs of the NLR. They are accelerated outwards by one of the mechanisms listed above. In the process, they develop significant micro-turbulence, which also serves to maintain them against disruption. As the clouds move outwards, the mechanism which generates the turbulence becomes weaker, which could be due the $1/r^2$ dilution of the radiation, or a drop in density of a wind. The dissipative heating would decrease, and there would be less enhancement of these emission-line ratios, as is observed (see Figures 1 – 3).

6. Summary

We have explored the effects of micro-turbulence and associated dissipative heating on emission-line ratios for conditions applicable to the NLR of Seyfert galaxies. Based on our modeling results, we suggest the following:

1. Micro-turbulence can increase the effect of photo-excitation, thereby boosting the relative strengths of resonance lines such as N V $\lambda 1240$. Turbulence alone will not directly affect collisionally excited, forbidden lines, such as [Ne V] $\lambda 3426$. However, we find that, if the turbulence dissipates over scale-lengths equal to the physical depths of the emission-line clouds, the resulting heating is sufficient to explain the highest [Ne V]/He II ratios detected in these spectra.

2. Although we found that the elemental abundances may be slightly super-solar, when turbulence and heating are included, there is no need to invoke higher abundances to explain the observed line ratios.

3. Although we cannot rule out that the emission-line widths may partly be due to super-position of kinematic components, the correlation between the line ratios and FWHM suggests that the clouds are turbulent and that the turbulence affects the relative strengths of the emission lines. This is further supported by the fact that including micro-turbulence of the same order of magnitude as the observed line widths can alleviate discrepancies between the models and the observations. While the turbulence appears to diminish with radial distance, the fact that the line widths exceed thermal throughout the inner ~ 200 pc of the NLR suggests that some process maintains the turbulence over large distances.

4. Micro-turbulence can make the clouds robust to the instabilities generated during

cloud acceleration. This suggests that the lifetime of non-turbulent clouds in the inner NLR may be brief. Hence, it may not be a coincidence that the emission and absorption lines observed in Seyfert galaxies have widths that far exceed their thermal widths.

In this paper, we have not attempted to fully explore the range of parameters, i.e., density, ionization, elemental abundances, and dust/gas ratio, that may exist in the NLR of Seyferts. Instead, we simply attempted to gauge the effects of turbulence/heating. In future work, it will be critical to examine the origins of the turbulence and develop a more sophisticated model for the dissipative heating, in particular regarding scale-lengths and the effects of internal magnetic field. In the meantime, these results suggest that it would be appropriate to include an approximation of turbulence/heating in photo-ionization studies of AGN. In a future paper, we plan to re-analyze the STIS long-slit spectra of NGC 1068 and explore the role of turbulence in detail.

This research has made use of NASA’s Astrophysics Data System. We thank Gary Ferland for his continued efforts in developing and upgrading the photoionization code Cloudy. We thank Bruce Woodgate and Fred Bruhweiler for useful discussions. We thank an anonymous referee for their useful comments.

REFERENCES

- Allen, A.J. 1984, MNRAS, 210, 147
- Arav, N., et al. 2007, ApJ, 658, 829
- Antonucci, R.R.J. 1993, ARA&A, 31, 473
- Armentrout, B.K., Kraemer, S.B., & Turner, T.J. 2007, ApJ, in press
- Asplund, M., Grevesse, N., & Sauval, A.J. 2005, in ASP Conference Series 336, Cosmic Abundances as Records of Stellar Evolution and Nucleosyntheses, ed. T.G. Barnes, III, & F.N. Bash (San Francisco:ASP), 25
- Blandford, R.D. & Payne, D.G. 1982, MNRAS, 199,883
- Bottoff, M.C., & Ferland, G.J. 2000, MNRAS, 316, 103
- Bottoff, M.C., & Ferland, G.J. 2002, ApJ, 568, 581 (BF2002)
- Bottoff, M. C., Korista, K.T., & Sholsman, I. 2000, ApJ, 537, 134
- Blumenthal, G.R., & Mathews, W.G. 1975, ApJ, 198, 517
- Collins, N.R., Kraemer, S.B., Crenshaw, D.M., Ruiz, J.R., Deo, R., & Bruhweiler, F.C. 2005, ApJ, 619, 116

- Crenshaw, D.M., & Kraemer, S.B. 1999, *ApJ*, 521, 572
- Crenshaw, D.M., & Kraemer, S.B. 2000, *ApJ*, 532, L101
- Crenshaw, D.M. & Kraemer, S.B. 2005, *ApJ*, 625, 680
- Crenshaw, D.M., Kraemer, S.B., Boggess, A., Maran, S.P., Mushotzky, R.F., & Wu, C.-C. 1999, *ApJ*, 516, 750
- Crenshaw, D.M., Kraemer, S.B., & George, I.M. 2003, *ARA&A*, 41, 117
- Crenshaw, D.M., et al. 1996, *ApJ*, 470, 322
- Crenshaw, D.M., Kraemer, S.B., Hutchings, J.B., Bradley, L.D. II, Gull, T.R., Kaiser, M.E., Nelson, C.H., Ruiz, J.R., & Weistrop D. 2000, *AJ*, 120, 1731
- Crenshaw, D.M., Kraemer, S.B., Hutchings, J.B., Danks, A.C., Gull, T.R., Kaiser, M.E., Nelson, C.H., & Weistrop, D. 2000, *ApJ*, 545, L27
- Das, V., Crenshaw, D.M., Hutchings, J.B., Deo, R.P., Kraemer, S.B., Gull, T.R., Kaiser, M.E., Nelson, C.H., & Weistrop, D. 2005, *AJ*, 130, 945
- Das, V., Crenshaw, D.M., & Kraemer, S.B. 2007, *ApJ*, 656, 699
- Das, V., Crenshaw, D.M., Kraemer, S.B., & Deo, R. 2006, *AJ*, 132, 620
- Davidson, K., & Netzer, H. 1979, *Rev. Mod. Physics*, 51, 715
- Delahaye, F., & Pinsonneault, M.H., 2006, *ApJ*, 649, 529
- Dietrich, M., Wagner, S.J., & Courvoisier, T.J.L. 1999, in *ASP Conf. Ser. 175, Structure and Kinematics of Quasar Broad Line Regions*, ed. C.M. Gaskell, W.N. Brandt, M. Dietrich, D. Dultzin-Hacyan, & M. Eracleous (San Francisco: ASP), 1
- Dunn, J.P., Crenshaw, D.M., Kraemer, S.B., & Gabel, J.R. 2007, *AJ*, in press
- Everett, J.E., & Murray, N. 2007, *ApJ*, 656, 93
- Ferland, G.J., Korista, K.T., Verner, D.A., Ferguson, J.W., Kingdon, J.B., & Verner, E.M. 1998, *PASP*, 110, 749
- Hutchings, J.B., et al. 1998, *ApJ*, 492, L115
- Grevesse, N., & Anders, E. 1989, in *AIP Conf. Proc. 183, Cosmic Abundances of Matter*, ed. C.J. Waddington (New York:AIP), 1
- Grevesse, N., & Sauval, A.J. 1998, *Space, Sci. Rev.*, 85, 161
- Groves, B.A., Dopita, M.A., & Sutherland, R.S. 2004, *ApJS*, 153, 9
- Khachikian, E. Ye., & Weedman, D.W. 1971, *Astrofizika*, 7, 389
- Kinkhabwala, A., Sako, M., Behar, E., Kahn, S.M., Paerels, F., Brinkman, A.C., Kaastra, J.S., Gu, M.F., & Liedahl, D.A. 2002, *ApJ*, 575, 732

- Koski, A.T. 1978, *ApJ*, 223, 56
- Kraemer, S.B., & Crenshaw, D.M. 2000a, *ApJ*, 532, 256
- Kraemer, S.B., & Crenshaw, D.M. 2000b, *ApJ*, 544, 763
- Kraemer, S.B., Crenshaw, D.M., Filippenko, A.V., & Peterson, B.M. 1998a, *ApJ*, 499, 719
- Kraemer, S.B., Crenshaw, D.M., & Gabel, J.R. 2001, *ApJ*, 557, 30
- Kraemer, S.B., Crenshaw, D.M., Hutchings, J.B., Gull, T.R., Kaiser, M.E., Nelson, C.H., & Weistrop, D. 2000, *ApJ*, 531, 278
- Kraemer, S.B., Crenshaw, D.M., Hutchings, J.B., Danks, A.C., Gull, T.R., Kaiser, M.E., Nelson, C.H., & Weistrop, D. 2001, *ApJ*, 551, 671
- Kraemer, S.B., & Harrington, J.P. 1986, *ApJ*, 307, 478
- Kraemer, S.B., Ho, L.C., Crenshaw, D.M., Shields, J.C., & Filippenko, A.V. 1999, *ApJ*, 520, 564
- Kraemer, S.B., Ruiz, J.R., & Crenshaw, D.M. 1998b, *ApJ*, 508, 232
- Kraemer, S.B., et al. 2005, *ApJ*, 633, 693
- Krolik, J.H., & Kriss, G.A. 2001, *ApJ*, 561, 684
- Krolik, J.H., McKee, C.F., & Tarter, C.B. 1981, *ApJ*, 249, 422
- Kwan, J., & Krolik, J.H. 1981, *ApJ*, 250, 478
- Marscher, A.P. 1978, *ApJ*, 225, 725
- Mathews, W.G. 1976, *ApJ*, 207, 351
- Minter, A.H., & Balseer, D.S. 1997, *ApJ*, 484, L133
- Nelson, C.H., Weistrop, D., Hutchings, J.B., Crenshaw, D.M., Gull, T.R., Kaiser, M.E., Kraemer, S.B., & Lindler, D. 2000, *ApJ*, 531, 275
- Oke, J.B., & Sargent, W.L.W. 1968, *ApJ*, 151, 807
- Oliva, E. 1997, in *ASP Conf. Ser. 113, Emission Lines in Active Galaxies: New Methods and Techniques*, ed. B.M. Peterson, F.-Z. Cheng, & A.S. Wilson (San Francisco: ASP), 288
- Osterbrock, D.E., 1989, *Astrophysics of Gaseous Nebulae and Active Galactic Nuclei* (Mill Valley: University Science Books)
- Peterson, B.M., et al. 2004, *ApJ*, 613, 682
- Ruiz, J.R., Crenshaw, D.M., Kraemer, S.B., Bower, G.A., Gull, T.R., Hutchings, J.B., Kaiser, M.E., & Weistrop D. 2001, *AJ*, 122, 2961

- Ruiz, J.R., Crenshaw, D.M., Kraemer, S.B., Bower, G.A., Gull, T.R., Hutchings, J.B., Kaiser, M.E., & Weistrop D. 2005, *AJ*, 129, 73
- Sako, M., Kahn, S.M., Paerels, F., & Liedahl, D.A. 2000, *ApJ*, 543, L115
- Schiano, A.V.R. 1986, *ApJ*, 302, 95
- Schmitt, H.R., Donley, J.L., Antonucci, R.R.J., Hutchings, J.B., & Kimmey, A.L. 2003, *ApJS*, 148, 327
- Schmitt, H.R., & Kinney, A.L. 1996, *ApJ*, 463, 498
- Smith, S.J. 1993, *ApJ*, 411, 570
- Stone, J.M., Ostriker, E.C., & Gammie, C.F. 1998, *ApJ*, 508, L99
- Turner, T.J., Kraemer, S.B., Mushotzky, R.F., George, I.M., & Gabel, J.R. 2003, *ApJ*, 594, 128
- Vila-Costas, M.B., & Edmunds, M.G. 1993, *MNRAS*, 265, 199
- Weymann, R.J., Scott, J.S., Schiano, A.V.R., & Christiansen, W.A. 1982, *ApJ*, 262, 497
- Wilson, A.S., & Raymond, J.C. 1999, *ApJ*, 513, L115
- Woodgate, B.E., et al. 1998, *PASP*, 110, 1183

Table 1. Model Parameters^a

Turbulence Velocity (km s ⁻¹)	Heating ^b (ergs s ⁻¹ cm ⁻³)
50	2.9×10^{-15}
100	2.3×10^{-14}
150	7.8×10^{-14}
200	1.8×10^{-13}
250	3.6×10^{-13}

^aFor the set of models, we assumed $N_H = 10^{21}$ cm⁻², $n_H = 10^5$ cm⁻³, and the elemental abundances listed in Section 2.1

^bFor comparison, the radiative heating is 9.5×10^{-14} ergs s⁻¹ cm⁻³ and 1.1×10^{-13} ergs s⁻¹ cm⁻³, for $\log(U) = -1.5$ and -1.0 , respectively.

Fig. 1.— Dereddened NV $\lambda 1240$ /He II $\lambda 1640$ ratios measured in *HST*/STIS long-slit spectra of NGC 1068 (Kraemer & Crenshaw 2000a, 2000b) as a function of radial distance projected onto the plane of the sky (top panel) and FWHM (bottom panel). The filled and unfilled squares are from blue- and red-shifted knots, respectively. Note the increase in the line ratios with increasing FWHM.

Fig. 2.— Dereddened C IV $\lambda 1550$ /He II $\lambda 1640$ ratios for NGC 1068.

Fig. 3.— Dereddened [Ne V] $\lambda 3426$ /He II $\lambda 1640$ ratios for NGC 1068.

Fig. 4.— Selected fractional ionic abundances as a function of column density for an ionization parameter $\log(U) = -1.0$. Note that the fractions of N^{+4} and Ne^{+4} become negligible for $\log N_H > 21.5$, at which point the gas has become optically thick above the He II Lyman limit.

Fig. 5.— The ratio of N V $\lambda 1240$ /He II $\lambda 1640$ as a function of U , for micro-turbulence velocities $v = 0$ (solid line), 50 (long-dash), 100 (dash triple-dot), 150 (dash-dotted) 200 (short-dashed), and 250 (dotted) km s^{-1} . Dissipative heating was not included in these models, hence the enhancement of the N V is results solely from photo-excitation.

Fig. 6.— Same as Figure 5, but dissipative heating has been incorporated in the models (see Table 1.). Note that 1) the maximum N V/He II ratio predicted is a factor of nearly 3 times that for the turbulence-only models, and 2) the peak shifts to lower values of U as a function of v , as a result of the increased dissipative heating at high turbulence velocities.

Fig. 7.— Same as Figure 6, showing the [Ne V] $\lambda 3426$ /He II $\lambda 1640$ ratio. As noted in the text, for the densities and elemental abundances used in these models, [Ne V]/He II ratios $>$ unity require the heating predicted for $v > 100 \text{ km s}^{-1}$.

Fig. 8.— Thermal stability curves for our set of model parameters. The three curves are: no turbulence (solid line), $v_t = 150 \text{ km s}^{-1}$ (dotted line), and $v_t = 250 \text{ km s}^{-1}$ (dashed line). The asterisks correspond to $\log(U) = -1.4$, at which [Ne V]/He II peaks, and the crosses correspond to $\log(U) = 0.0$

Fig. 9.— Predicted N V $\lambda 1240$ /He II $\lambda 1640$ versus [Ne V] $\lambda 3426$ /He II $\lambda 1640$ are shown for models including dissipative heating for turbulence velocities 50 (dotted), 100 (dashed), and 150 (dash-dotted) km s^{-1} . The curves are generated for a range of ionization parameters $-2.0 \leq \log(U) \leq 0.0$, running counterclockwise, with the $\log(U)$ values marked at several points for the $v_t = 100$ and 150 km s^{-1} models. The observed ratios are from our previous NLR studies; the symbols from the different datasets are NGC 4151, crosses (Kraemer et al. 2000), NGC 1068, asterisks (Kraemer & Crenshaw 2000b), Mrk 3, squares (Collins et

al. 20005), NGC 5548, triangle (Kraemer et al. 1998a), and the NGC 1068 “Hot Spot”, diamond (Kraemer & Crenshaw 2000a).

Fig. 10.— Predicted N V $\lambda 1240$ /He II $\lambda 1640$ versus C IV $\lambda 1550$ /He II $\lambda 1640$ are shown for models including dissipative heating. Symbols are as described in Figure 9.

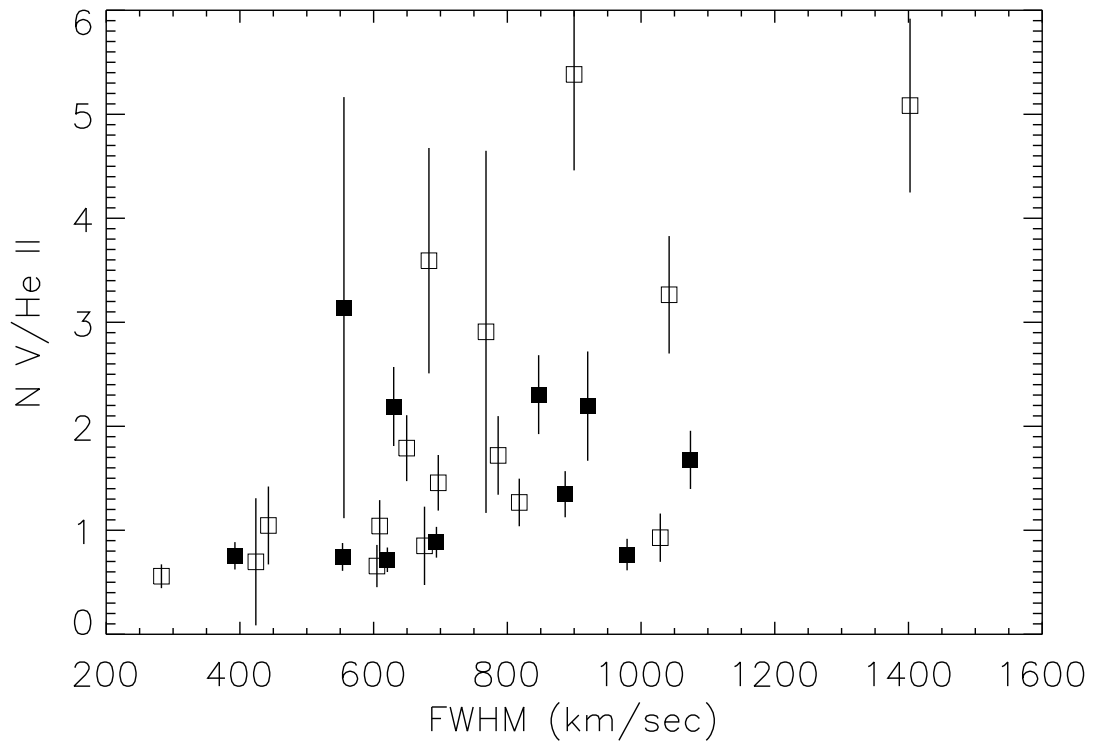
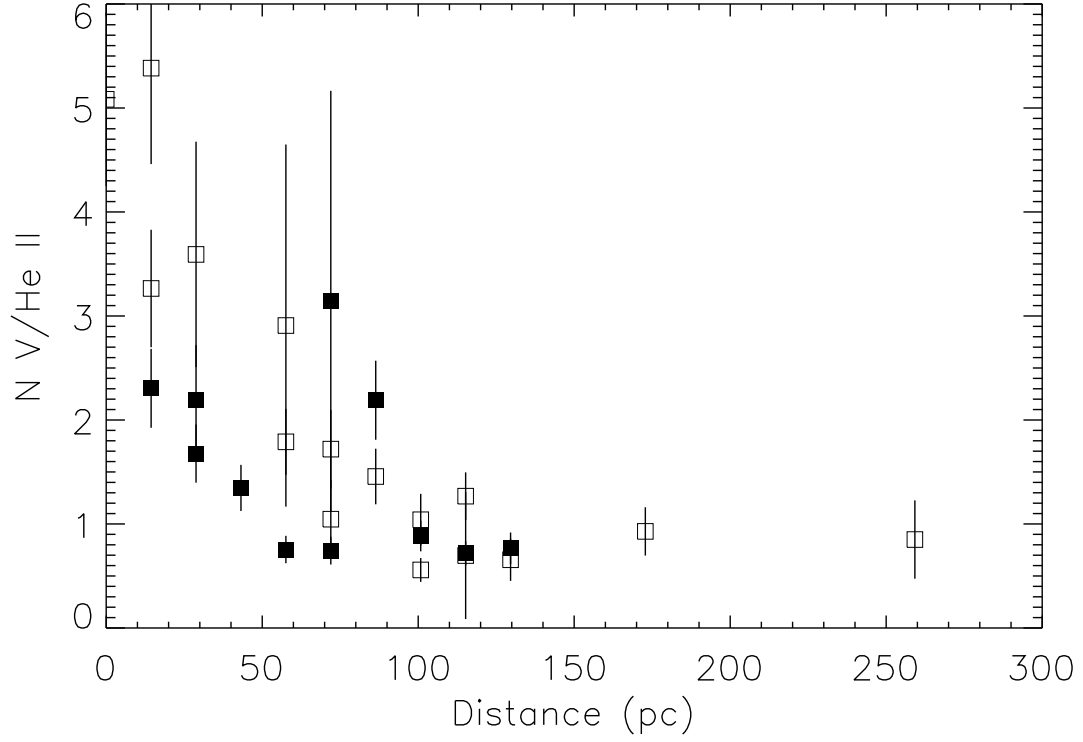


Fig. 1.

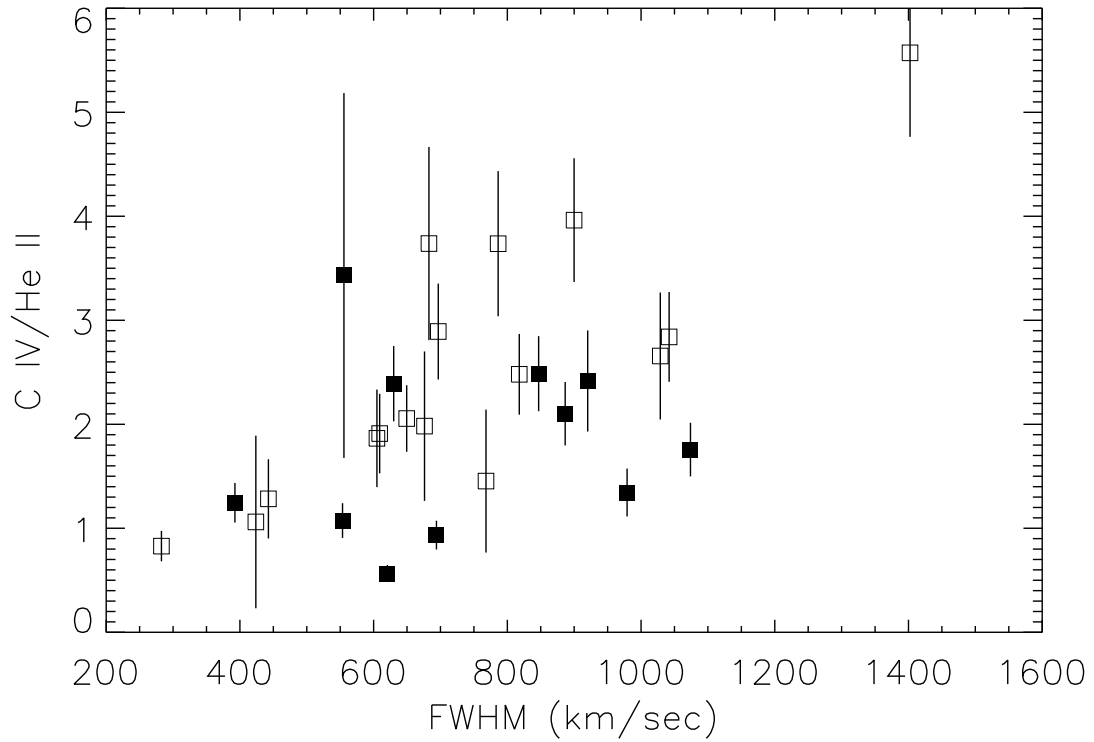
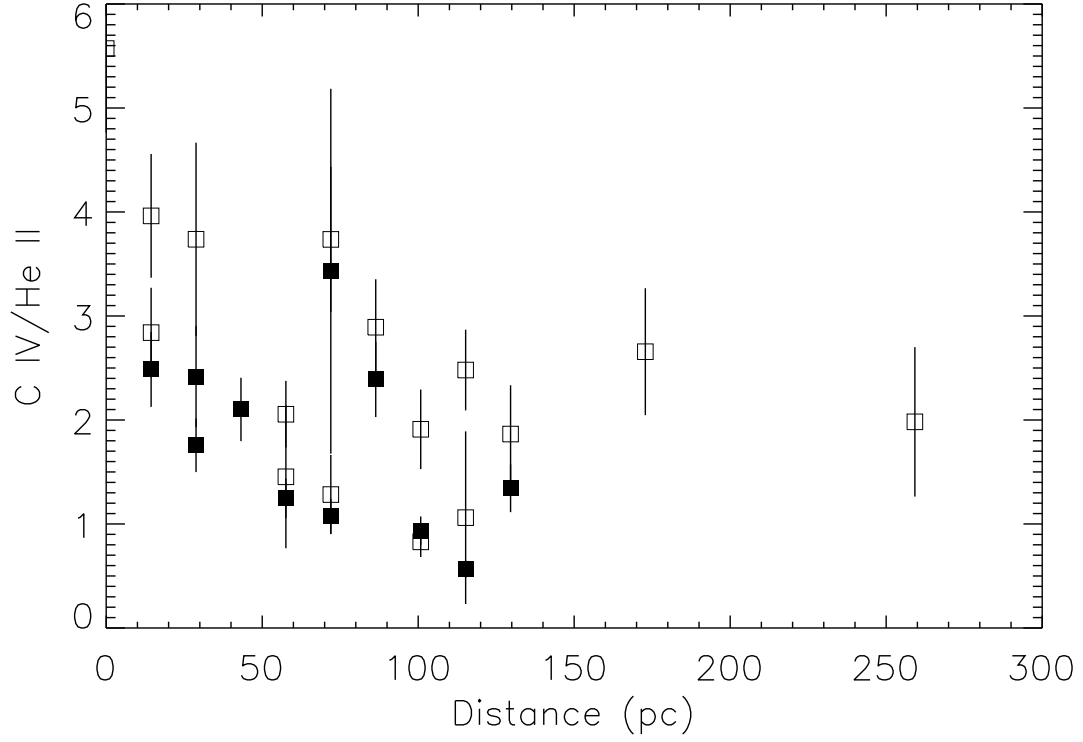


Fig. 2.

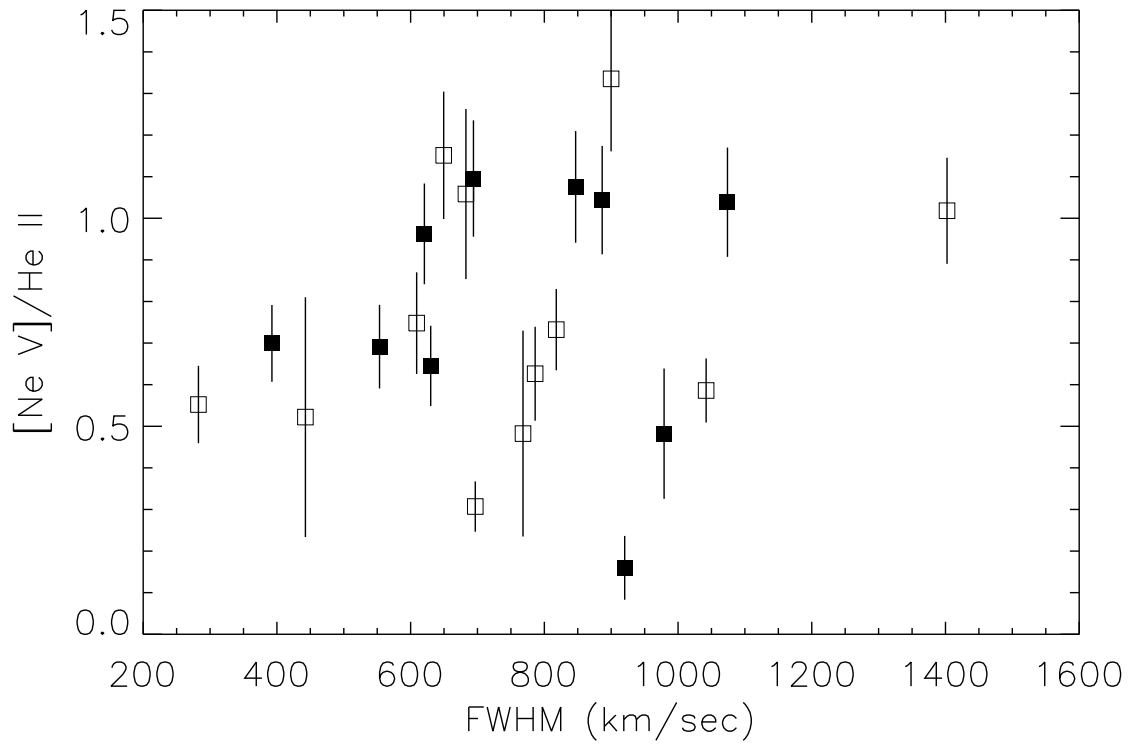
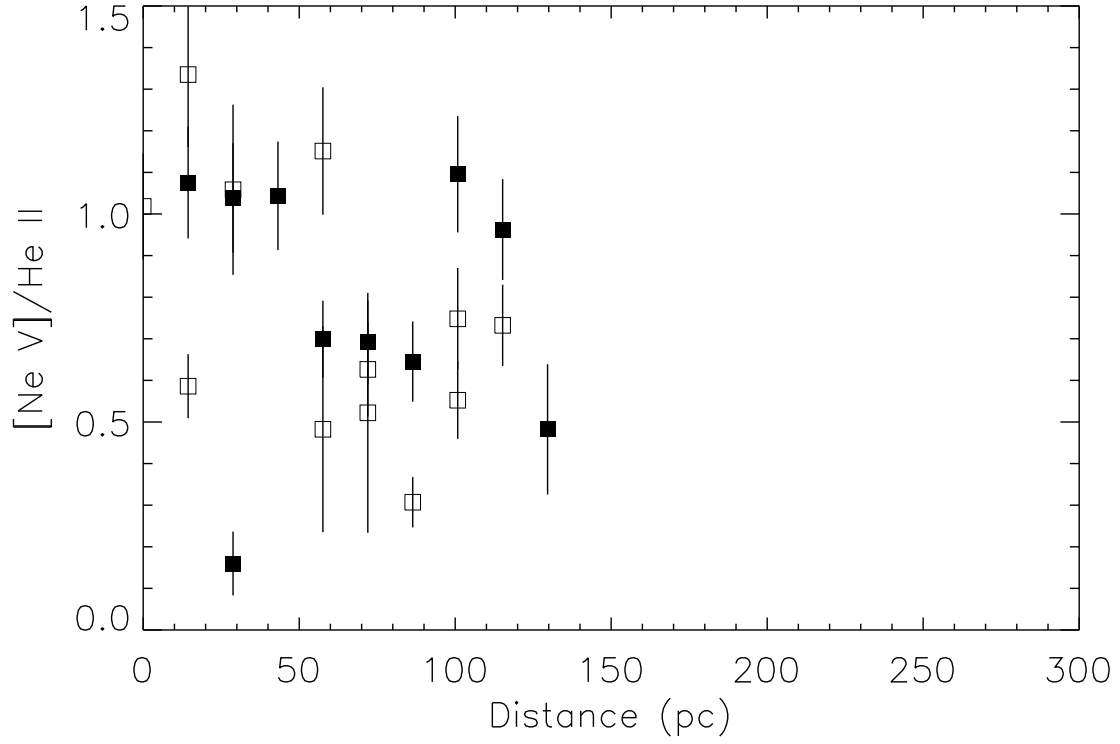


Fig. 3.

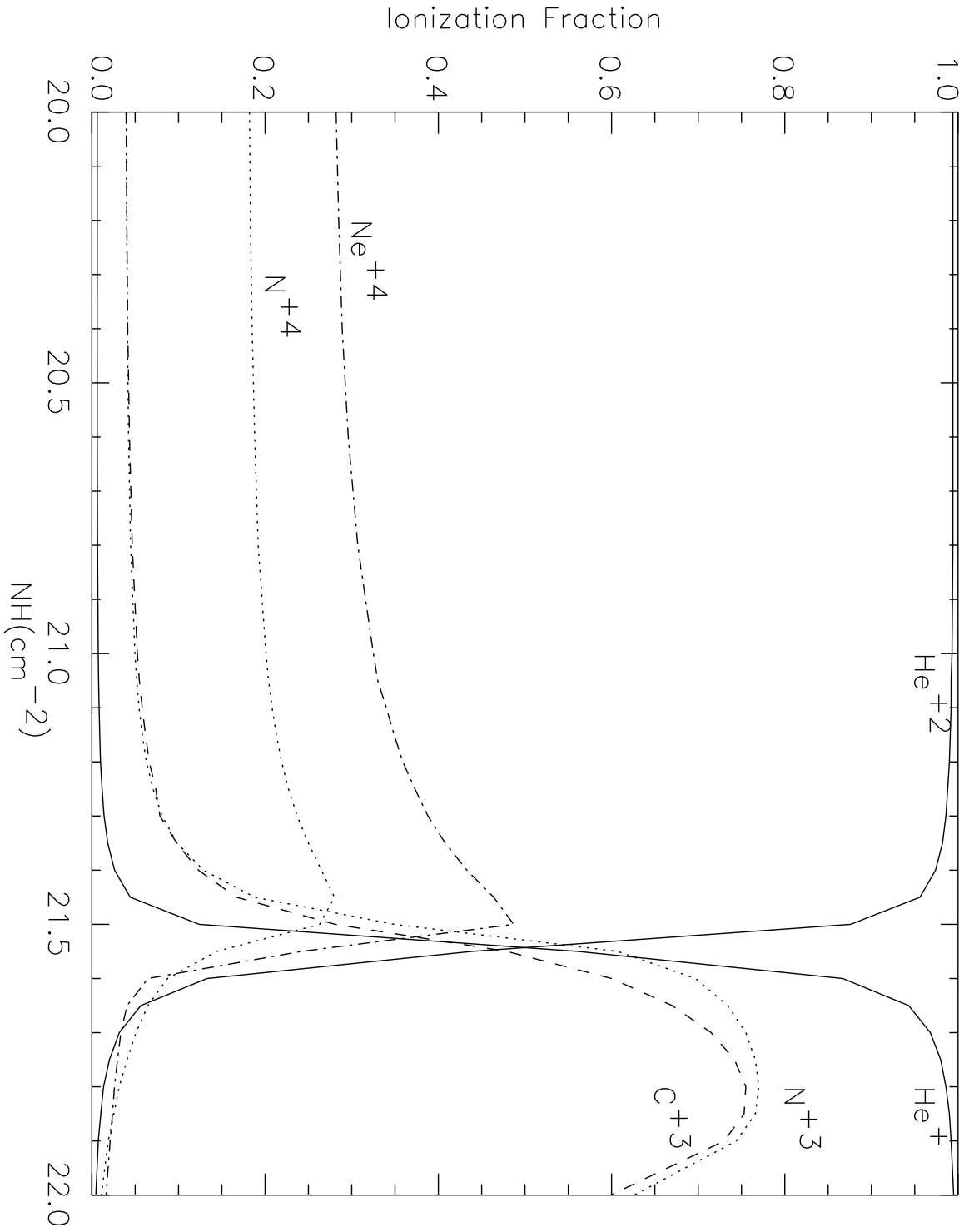


Fig. 4.

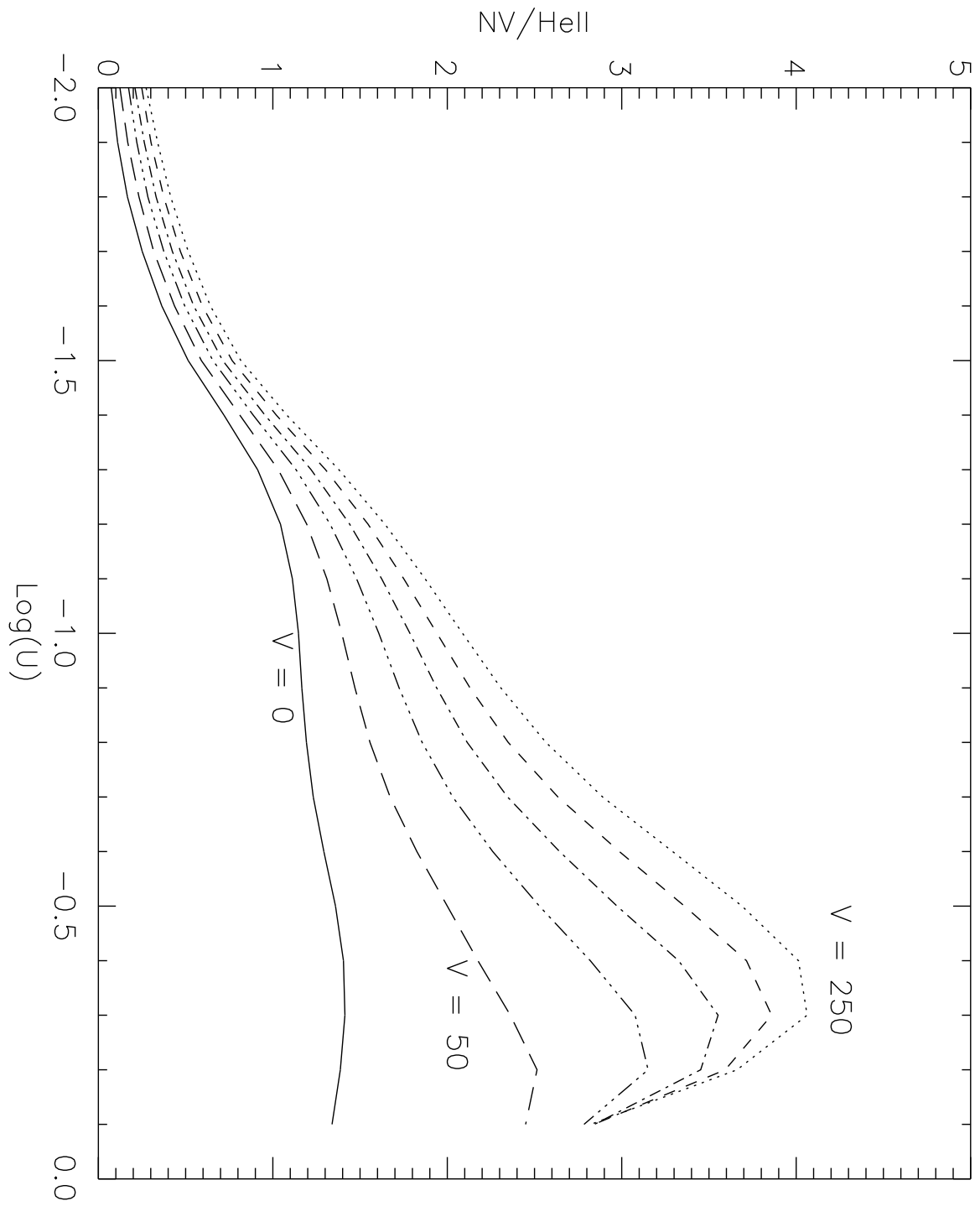


Fig. 5.

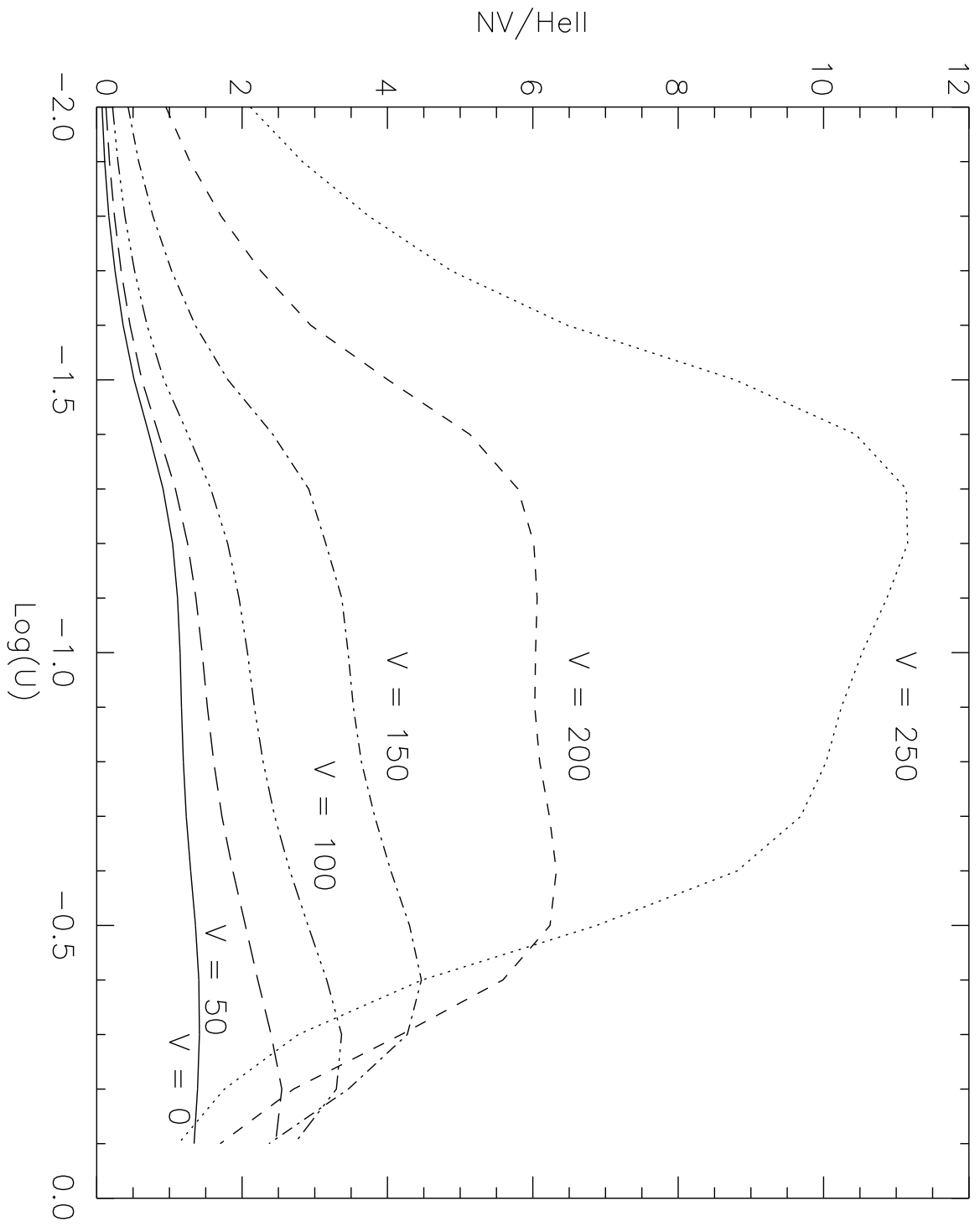


Fig. 6.

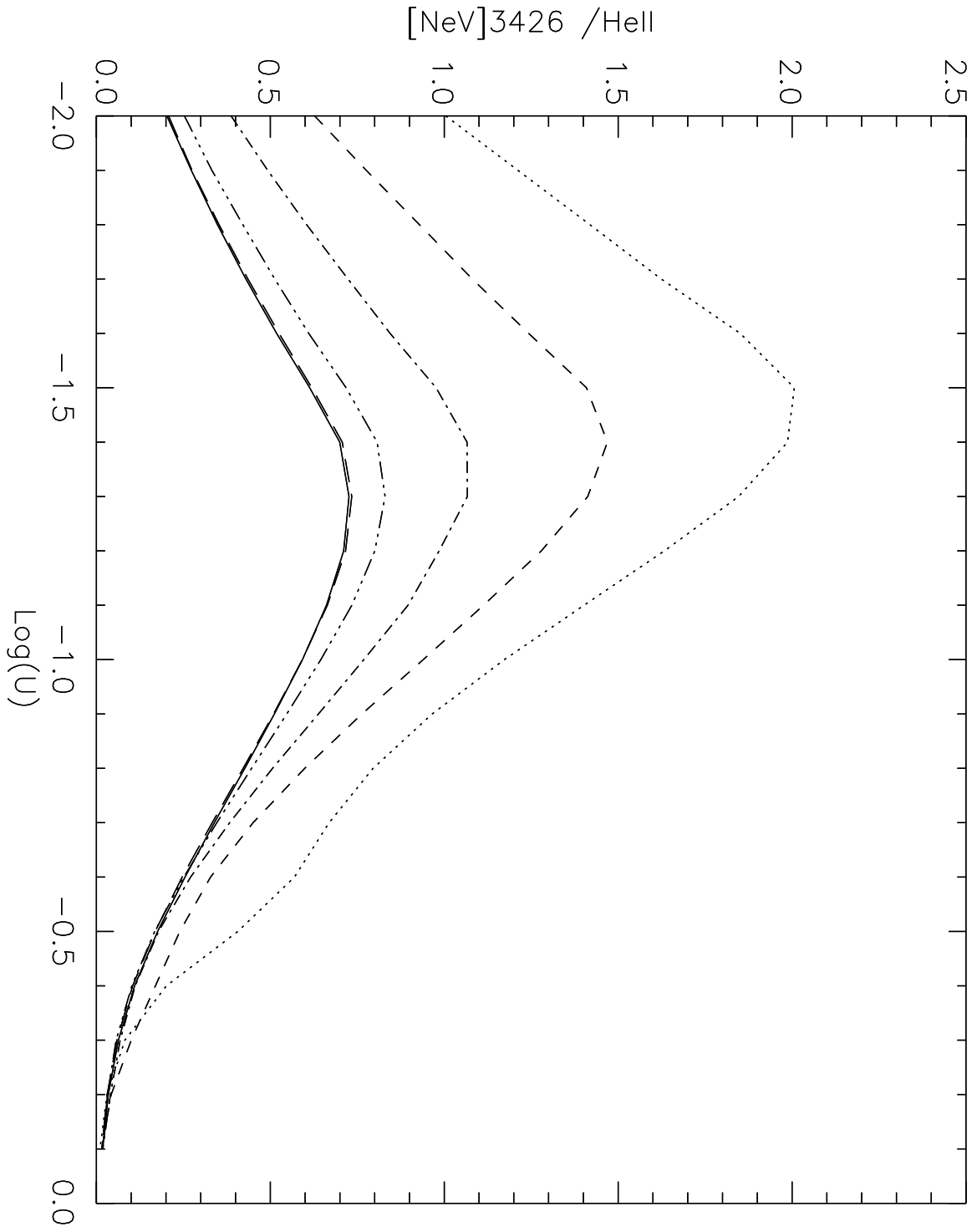


Fig. 7.

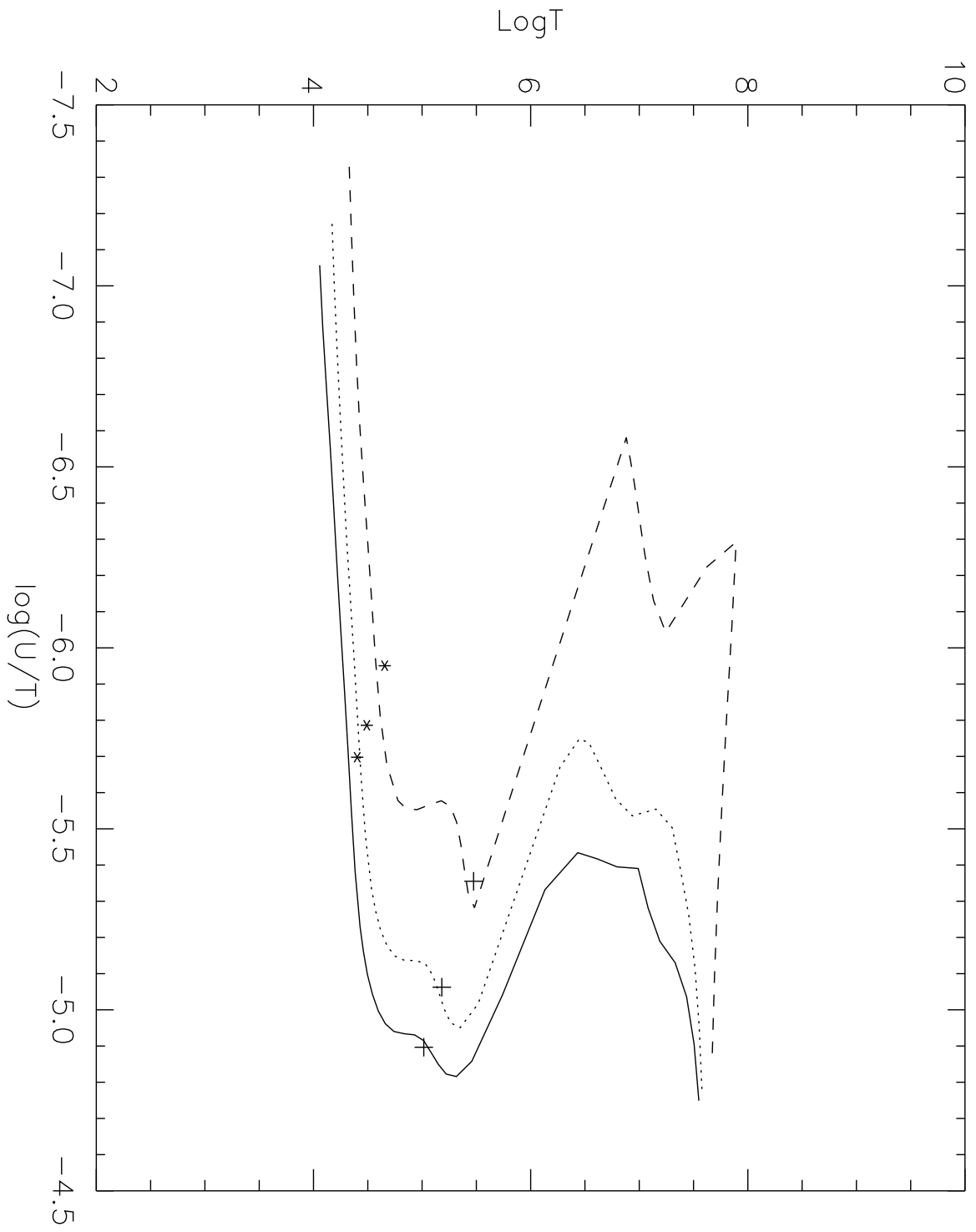


Fig. 8

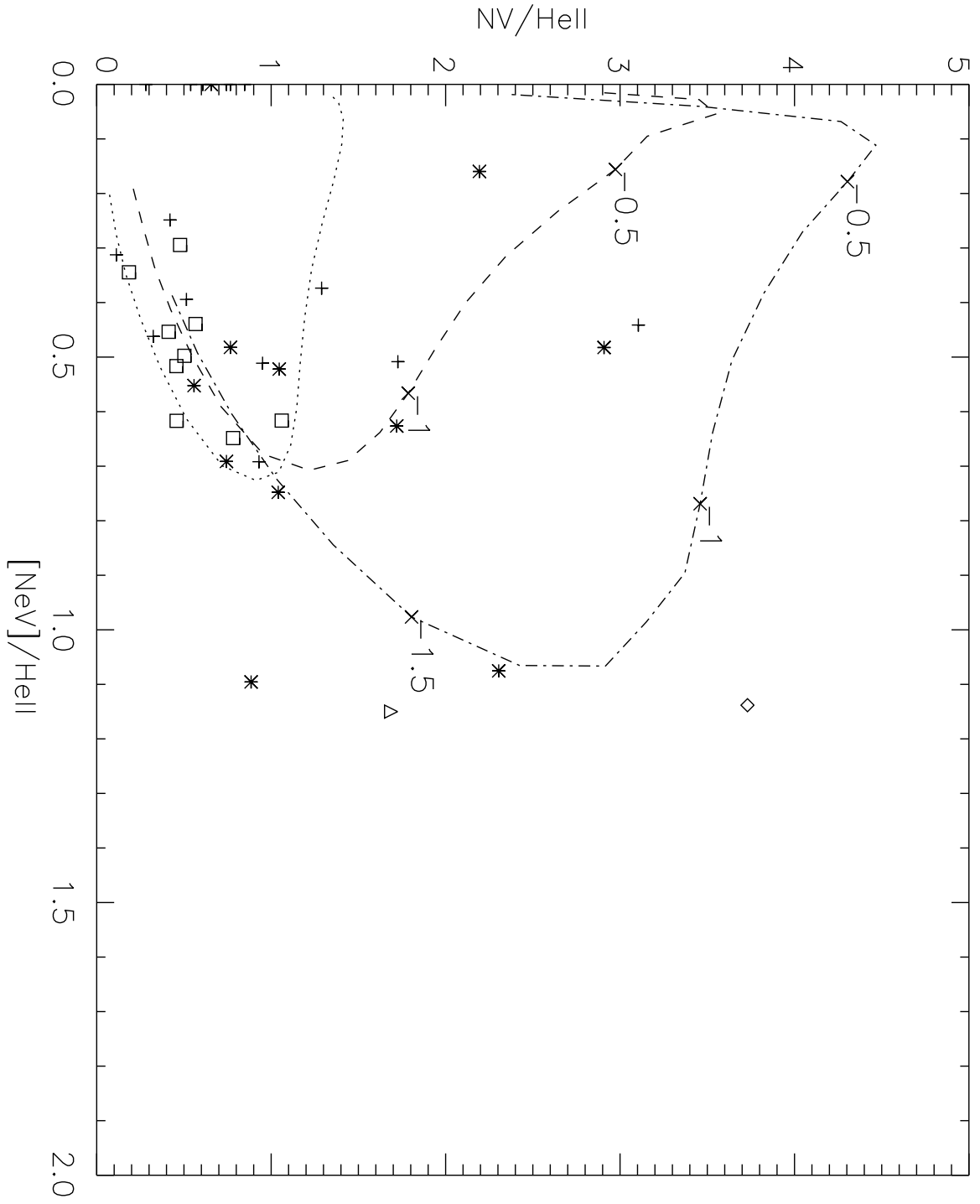


Fig. 9.

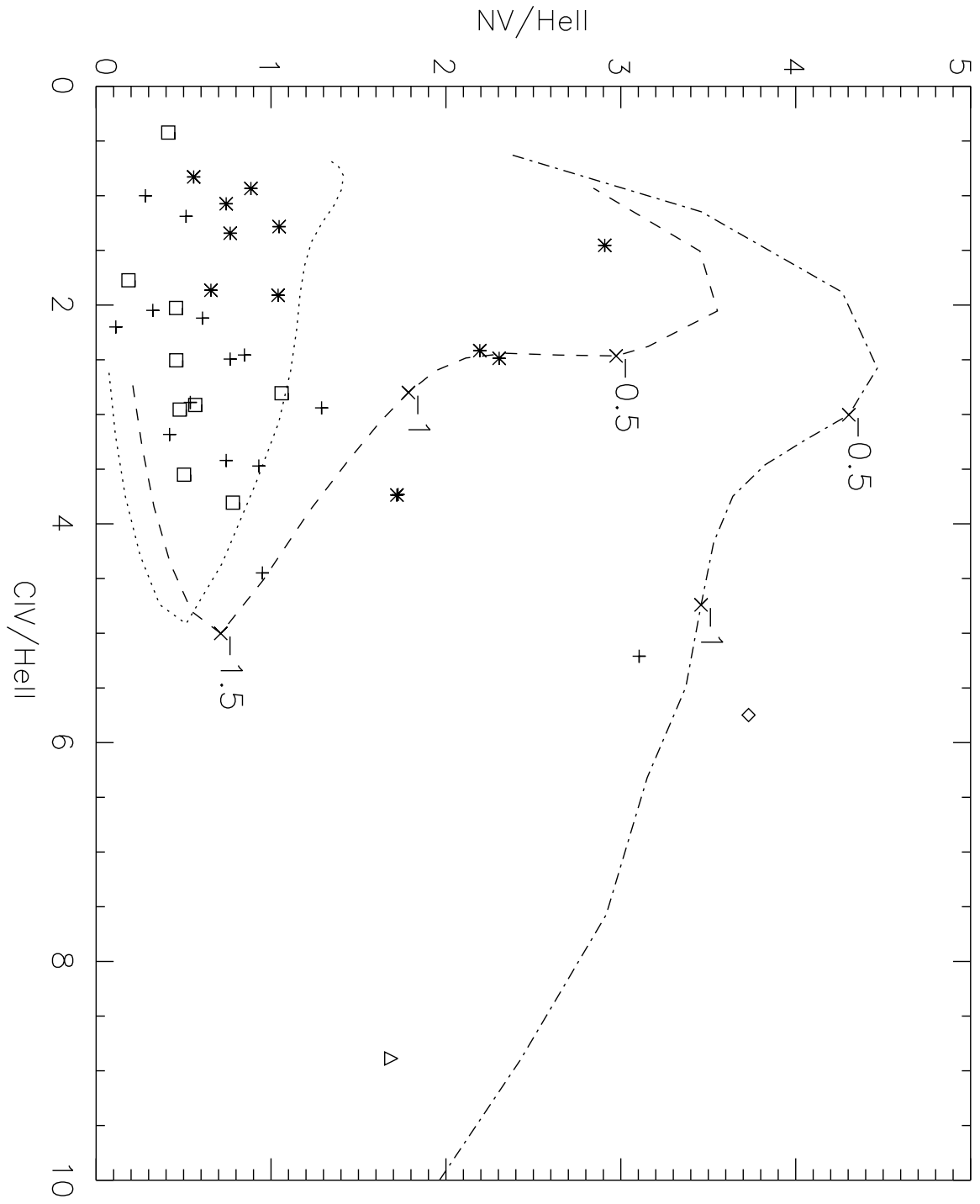


Fig. 10.